RSC Advances

COMMUNICATION

View Article Online
View Journal | View Issue

Cite this: *RSC Adv.*, 2014, **4**, 57218

Received 17th August 2014
Accepted 22nd October 2014

DOI: 10.1039/c4ra08790a

www.rsc.org/advances

Temperature and concentration dependent crystallization behavior of $Ge_2Sb_2Te_5$ phase change films: tungsten doping effects

Shuang Guo,[a] Zhigao Hu,*[a] Xinglong Ji,[b] Ting Huang,[a] Xiaolong Zhang,[a] Liangcai Wu,[b] Zhitang Song[b] and Junhao Chu[a]

Tungsten-doped $Ge_2Sb_2Te_5$ (GSTW) semiconductor films with W concentrations of 3.2, 7.1, and 10.8%, deposited by cosputtering, have been proposed to improve the crystallization behavior of $Ge_2Sb_2Te_5$ (GST) phase change materials. The crystalline resistances and crystallization temperatures of GST and GSTW films have been studied using *in situ* temperature-dependent resistance measurements. The intrinsic crystallization mechanism from amorphous to face-centered-cubic (FCC) structure has been discovered using temperature-dependent Raman spectra from 300 K to 720 K. It was found that GSTW films exhibit a more stable cubic geometry, better thermal stability of the amorphous state and higher 10 year data retention ability than pure GST. This could be due to the substitution of Te atoms or vacancies by W atoms in the crystal lattice, which leads to disorder of the crystalline structure and inhibits further crystallization.

1 Introduction

The phase change phenomenon was first proposed by Ovshinsky.[1] Because of the advantages of scalability, high recording density, high operation speed, high endurance and low power consumption, phase change random access memory (PRAM) has been recognized as one of the most promising candidates for next-generation nonvolatile memory devices.[2] Phase change materials based on chalcogenides have received much attention in recent years due to their unique characteristics in the fast transitions between the amorphous and crystalline phases upon heating.[3,4] Currently, Ge–Sb–Te, Ge–Te, and Sb–Te alloy systems have been deeply investigated owing to their superior phase change properties. Among them, the GeTe–Sb_2Te_3 pseudobinary compounds, especially $Ge_2Sb_2Te_5$ (GST) chalcogenide alloys, have been widely applied in commercial rewritable optical storage taking advantage of the rapid crystallization between amorphous GST (a-GST) and metastable cubic GST (c-GST).[5] However, pure GST also has some noticeable disadvantages: the relatively low crystallization temperature leading to a deteriorative amorphous thermal stability, the high melting point leading to a high power consumption, and so on.[6] Hence, it is necessary to find promising chalcogenide phase change materials to improve these properties. Two major methods have been applied in solving this interesting issue: (1) finding other phase change material systems such as Ge–Sb–Se, Si–Sb–Te, Ga–Sb–Te, Ge–Te and Sb–Te,[7–11] and (2) doping some elements into the original parent compound.

During the past few years, a number of elements have been doped into the conventional GST material to improve performance, such as nitrogen (N),[12] oxygen (O),[13] tin (Sn),[14] and silver (Ag).[15] Note that the W element is widely used in fundamental research and semiconductor industries. GST is very sensitive to W doping. A very small amount of W can obviously change the performance of GST, which could minimise phase separation. Based on the TEM images and the corresponding selected area electron diffraction (SAED) of GSTW films, the W atoms can uniformly distribute in the crystalline structure.[16] The atom radius of W is 139 pm, which is similar to that of Te (140 pm) and Sb (145 pm) atoms. It is supposed that most of the W atoms may act as substitutional impurities in the crystal lattice of GST.[17] On the other hand, W atoms are heavier than other dopant atoms. They can discourage the Ge, Sb, and Te atoms from further diffusion, which leads to a good endurance. Besides this, the electronegativity of W is relatively large, so the difference in electronegativity (ΔS) of Sb–Te is much smaller than that of W–Te. After substitution, the ΔS between Sb–Te and W–Te would give rise to a larger nucleation probability. For a growth-dominated material, this would significantly increase the phase change speed. Thus, GSTW has the potential to balance the operation speed and thermal stability.[17] Compared with PRAM based on GST, Cheng *et al.* proved a higher operation speed in a single PRAM cell based on GSTW (10 ns for

[a]*Key Laboratory of Polar Materials and Devices, Ministry of Education, Department of Electronic Engineering, East China Normal University, Shanghai 200241, China. E-mail: zghu@ee.ecnu.edu.cn; Fax: +86-21-54345119; Tel: +86-21-54345150*

[b]*State Key Laboratory of Functional Materials for Informatics, Shanghai Institute of Microsystem and Information Technology, Chinese Academy of Sciences, Shanghai 200050, China*

$W_{0.08}(Ge_2Sb_2Te_5)_{0.92}$ and 50 ns for GST) and that the cyclability is not decreased as a result of the W doping.[16] Moreover, when GSTW is applied in devices, contact with the W electrode is inevitable and will reduce the interface effect. However, the phase change mechanism of the W-doped GST system has not been presented to date.

The aim of this communication is to investigate the thermal stability and data retention ability of W-doped GST (GSTW). Importantly, the physical mechanism of GSTW has been systematically studied with the aid of temperature-dependent Raman scattering.

2 Experimental section

GST and GSTW films with a thickness of about 150 nm were prepared by cosputtering pure stoichiometric GST and elemental W on SiO_2/Si (100) substrates at room temperature. The concentrations of W dopant atoms in the GSTW films, examined by means of Energy Dispersive Spectroscopy (EDS), were confirmed to be 3.2 at%, 7.1 at%, and 10.8 at% (named GSTW3.2%, GSTW7.1%, and GSTW10.8%, respectively). The sheet resistance (R_s) of the films as a function of temperature was measured *in situ* using a Linkam T95 hot stage at a fixed heating rate of 40 K min^{-1}. The isothermal change in resistance with increasing temperature was used to judge the data retention ability of the amorphous films. Temperature dependent Raman scattering experiments were implemented using a Jobin-Yvon LabRAM HR 800 micro-Raman spectrometer and a THMSE 600 heating/cooling stage (Linkam Scientific Instruments) at a fixed heating rate of 10 K min^{-1} over the temperature range from 300 K to 720 K. The films were excited using a 488 nm Ar^+ laser at a power of 5 mW. The spectra were recorded in the back-scattering geometry with a resolution better than 1 cm^{-1}. The laser beam was focused through a 50× microscope with a working distance of 18 mm. An air-cooled charge coupled device (CCD) (−70 °C) with a 1024 × 256 pixels front illuminated chip was utilized to collect the scattered signal dispersed on a grating with 1800 grooves per mm.

3 Results and discussion

The *in situ* temperature dependent resistance (*R*–*T*) measurements of the GST and GSTW films were carried out to describe the sheet resistance change during the heating and cooling process as shown in Fig. 1(a). The R_s of all the films decreases gradually in the initial heating stage, which indicates that both GST and GSTW possess semiconducting characteristics. When the heating temperature reaches the crystallization temperatures (T_c), a sharp decrease in resistance is displayed, which can be associated with the change from amorphous to face-centered-cubic (FCC) structure. The FCC structure is a metastable state for the GST film, while it is a stable state for the GSTW films.[16] Another sharp decrease in resistance for the GST film is observed around 640 K, which could be due to the conversion from the metastable FCC to a hexagonal (HEX) structure. The T_c values from amorphous to FCC structure can be estimated to be 435, 456, 493, and 550 K for the GST, GSTW3.2%, GSTW7.1%, and GSTW10.8% films, respectively. The T_c shifts to a higher temperature with increasing W concentration. It can be concluded that the W dopant could suppress the crystallization. A suitably higher T_c will be beneficial for improving the thermal stability of the amorphous films, which is helpful for the data retention ability. In addition, it can be observed that the crystalline resistance of GSTW is higher than that of pure GST during the cooling stage, which can result in a low reset power consumption in PRAM devices.

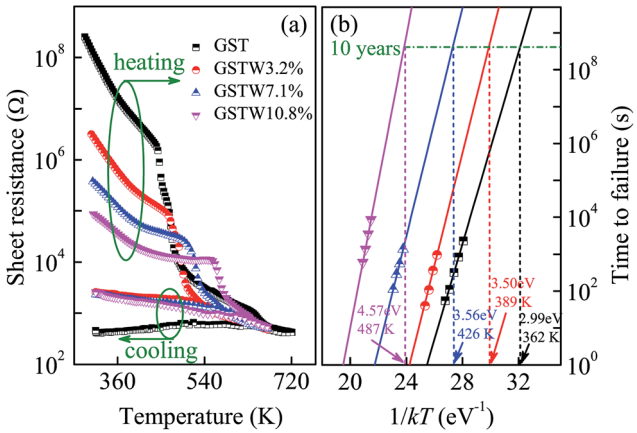

Fig. 1 (a) Sheet resistance as a function of temperature for GST and GSTW films with a heating rate of 40 K min^{-1}. (b) The Arrhenius extrapolation at 10 year data retention for GST and GSTW films.

The thermal stability of the amorphous GST and GSTW films can be analyzed using the data retention and crystallization activation energy (E_a) derived from extrapolation of the isothermal Arrhenius plots.[18] The 10 year data retention temperature can be obtained using the Arrhenius equation: $t = \tau \times \exp(E_a/kT)$, where t is the failure time, τ is a proportional time constant, and k is Boltzmann's constant. The best-fitting result for the failure time *vs.* the reciprocal of isothermal temperature ($1/kT$) is shown in Fig. 1(b). The 10 year data retention temperatures of the amorphous GST, GSTW3.2%, GSTW7.1%, and GSTW10.8% films are 362 K, 389 K, 426 K, and 487 K, respectively. The E_a values are 2.99 eV, 3.50 eV, 3.56 eV, and 4.57 eV, respectively. Both the 10 year data retention ability and the crystallization activation energy are improved with increasing W concentration. Higher E_a means better thermal stability in PRAM devices. However, an excessively large E_a may lead to an ultra high reset power consumption. Kao *et al.* proposed that the storage requirement of data retention for automotive electronics is 10 years at 393 K.[19] Therefore, the 10 year data retention ability (426 K) of GSTW7.1% can satisfy this requirement.

The amorphous and crystalline geometrical structures of GST have been determined using *ab initio* molecular dynamics simulations.[20] Based on the analysis of X-ray absorption fine structure using electron excited X-ray appearance potential spectroscopy (EXAPS), Kolobov *et al.* proposed the geometry of a-GST and c-GST.[3,21] The GST compound can be regarded as having two constituents, namely GeTe and Sb_2Te_3. In a-GST, about one-third of the Ge atoms are in tetrahedral

coordination, and the majority of the Ge atoms and all the Te and Sb atoms are in defective octahedra.[22] However, GST can be regarded as having the rock salt geometry in the crystalline structure. The Te atoms occupy one sublattice and the Ge and Sb atoms and about 20% of the vacancies are placed in the other sublattice randomly.[23]

Raman scattering is sensitive to the change of coordination in local symmetry, which results from distortion and atomic substitution of polyhedra. Thus, Raman scattering can be used to analyze the detailed structural variation of the GST and GSTW films during the transition from amorphous to crystalline phase. Note that the W atoms may be considered as undergoing displacement doping in the crystal lattice of GST. Fig. 2 shows the Raman spectra of the GST and GSTW films with several characteristic temperatures from 340 K to 720 K. The main feature of the Raman spectra for the GST and GSTW films is a prominent broadening band covering the 60 cm^{-1} to 250 cm^{-1} frequency region. With increasing temperature, the GST film transforms from amorphous to metastable FCC structure and further crystallizes into a HEX structure. However, the GSTW films transform directly from amorphous to stable FCC structure. This indicates that W doping can restrain GST from further crystallization. The Raman spectra can be regarded as two broadening peaks marked with A and B, respectively, as shown in Fig. 2. The main feature of the Raman spectra for all four samples is that the intensity of peak A increases, while that of peak B decreases with increasing temperature. When the temperatures approach a certain value, peak B shifts to a higher frequency, whose value corresponds to the T_c data. The T_c from amorphous to FCC structure is estimated to be around 420, 435, 480, and 540 K for the GST, GSTW3.2%, GSTW7.1%, and GSTW10.8% films, respectively. The T_c shifts to a higher temperature with increasing W concentration, which is in good agreement with the above R–T measurements. Nevertheless, the T_c values from the Raman spectra are slightly lower than those from the R–T measurements. This can be attributed to the lower heating rate in the Raman scattering experiments. Besides this, peak B shifts to a lower frequency with increasing W concentration. The frequency of peak B decreases from 150 cm^{-1} to 145 cm^{-1} for the amorphous structure and from 165 cm^{-1} to 151 cm^{-1} for the crystalline structure. Due to the fact that W atoms are heavier than Te atoms, the redshift in frequency may be related to the substitution of Te atoms or vacancies by W atoms in the structure units.

The vibrational modes of a-GST films observed in Raman spectra can be attributed to defective octahedra, $GeTe_{4-n}Ge_n$ (n = 0, 1, 2) edge- and/or corner-sharing tetrahedra and $SbTe_3$ pyramidal units. For c-GST films, they can be attributed to defective octahedra, corner-sharing $GeTe_{4-n}Ge_n$ (n = 0, 1, 2) tetrahedra and hexagonal Sb_2Te_3.[24] To clarify the phase change mechanism, the Raman spectra were fitted with the aid of Gaussian oscillator model to quantitatively describe the vibrational modes. Fig. 3 depicts the representative fitted Raman spectra of the a-GST at 340 K and c-GST at 630 K. Six Gaussian oscillators can be labeled as peak 1, 2, 3, 4, 5, and 6, respectively.

In order to analyze the transition from amorphous to FCC, the assignment of phonon modes is necessary. The assignments of the phonon modes and the frequencies of each peak at 340 K and 630 K are listed in Table 1.[10,11,25,26] The two lower Raman peaks, namely peak 1 (~67 cm^{-1}) and peak 6 (200–210 cm^{-1}), can undoubtedly be assigned to the F_2 mode of the bending and antisymmetric stretching vibrations of the $GeTe_4$ tetrahedra, respectively. Peak 2 at about 88 cm^{-1} can be associated with the E mode of the $GeTe_4$ tetrahedra vibrations. Peak 3 at about 103 cm^{-1} can be related to the A_1 mode of the corner-sharing $GeTe_4$ tetrahedra vibrations. The vibrational modes of these four peaks are consistent in both amorphous and FCC geometries. However, peak 4 and 5 are different in the two structures. Peak 4 can be attributed to the A_1 mode of the $GeTe_{4-n}Ge_n$ (n = 1, 2) corner- and/or edge-sharing tetrahedra vibrations, and the E_g (2) mode of the Sb–Te band vibrations in

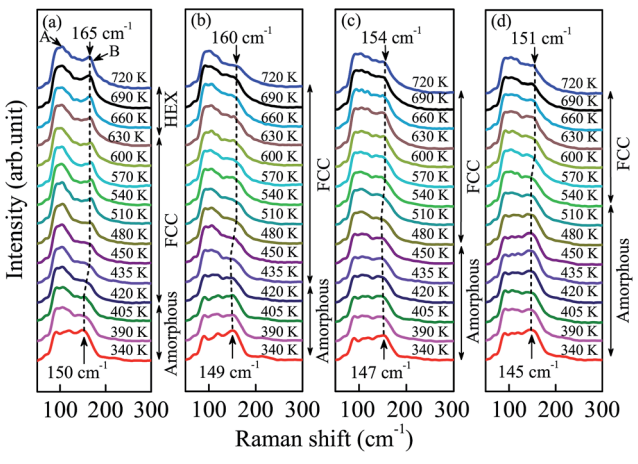

Fig. 2 Temperature dependence of Raman spectra for (a) GST, (b) GSTW3.2%, (c) GSTW7.1%, and (d) GSTW10.8% films from 340 K to 720 K. Note that the phase change characteristics are indicated by the dashed lines.

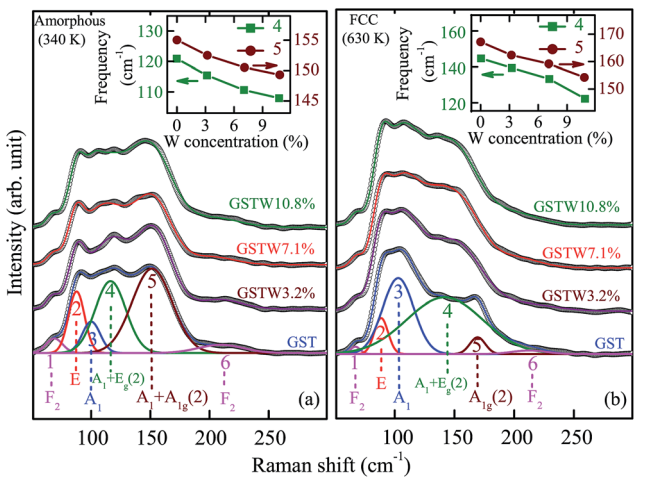

Fig. 3 Raman spectra of (a) a-GST at 340 K and (b) c-GST at 630 K with different W concentrations. Note that the best-fitting Raman spectra of a-GST and c-GST are shown. The insets show the frequency variations of peak 4 and peak 5 as a function of W concentration.

Table 1 The assignments of phonon modes fitted using Gaussian oscillators and the frequencies of each oscillator, recorded at 340 K (amorphous) and 630 K (FCC). Note that the unit of the frequencies is cm^{-1}

Geometry	Assignment	GST	GST3.2%	GST7.1%	GST10.8%
Amorphous	1 [F_2 $n = 0$ bending vibration]	67.4	67.3	68.1	67.9
	2 [E $n = 0$]	88.5	88.0	88.2	89.1
	3 [A_1 $n = 0$ corner-sharing]	107	106	102	102
	4 [$A_1 + E_g$ (2) $n = 1, 2$ corner-/edge-sharing]	121	115	111	108
	5 [$A_1 + A_{1g}$ (2) $n = 0$ edge-sharing]	155	153	151	148
	6 [F_2 $n = 0$ stretching vibration]	211	208	201	200
FCC	1 [F_2 $n = 0$ bending vibration]	67.1	67.6	67.7	67.0
	2 [E $n = 0$]	89.2	88.7	88.1	87.7
	3 [A_1 $n = 0$ corner-sharing]	103	102	103	102
	4 [$A_1 + E_g$ (2) $n = 1, 2$ corner-sharing]	145	136	133	122
	5 [A_{1g} (2)]	167	162	159	154
	6 [F_2 $n = 0$ stretching vibration]	213	210	200	200

the $SbTe_3$ pyramidal entities in the amorphous state. However, the $GeTe_{4-n}Ge_n$ ($n = 1, 2$) corner-sharing tetrahedra vibrational modes disappear in the FCC structure. It can also be confirmed that the defective octahedral Ge sites appear in both the amorphous and FCC structures. Peak 5 can be attributed to the A_1 mode of the $GeTe_4$ edge-sharing tetrahedra vibrations, and the A_{1g} (2) mode of the Sb–Sb band vibrations in $(Te_2)Sb–Sb(Te_2)$ or $(Te_2)Sb–Sb(TeSb)$ and similar structures in the amorphous state. However, only the A_{1g} (2) mode corresponding to the Sb–Sb band vibrations exists in the FCC structure, that is, the A_1 mode of the $GeTe_4$ edge-sharing tetrahedra vibrations disappears. According to the parameters in Table 1, we can conclude that the frequencies of peaks 1, 2, 3, and 6 change little with increasing temperature and W concentration, while the frequencies obviously change for peak 4 and peak 5. Note that a slight redshift in the frequency of peak 6 can be observed. Besides this, it can be seen from the inset of Fig. 3 that the frequencies of peak 4 and peak 5 decrease sharply with increasing W concentration. Because W atoms are heavier than Te atoms, the redshift in frequency may be due to the substitution of Te atoms by W atoms in the structural units corresponding to the vibrational modes of peaks 4, 5, and 6. It can be seen that the tetrahedral units also survive in the FCC structure. This phenomenon could be due to the slightly incomplete crystallization, which may be caused by the low heating rate.

It is known that the most prominent peaks in the Raman spectra are mainly caused by Sb_2Te_3 units, especially in the amorphous state. However, the GeTe component takes the main responsibility for the phase change in the GST film. It is easy to identify the phase transition from amorphous to crystalline structure from the evolutions of frequency and intensity of the phonon modes. Fig. 4 shows the frequency variations of peaks 4 and 5 of GSTW, and peaks 4, 5 and 6 of GST, as well as the strength variations of peaks 3 and 5 of GST and GSTW as a function of temperature. It can be seen that the frequency and intensity variational sections correspond to the phase change regions. This phenomenon can be attributed to the fact that the heavier W atoms prevent the GST elements from diffusing further and improve the degree of disorder of GSTW. Thus, the diffusion prevention and disorder suppress the crystallization of amorphous films, which contributes to a good endurance. At T_c, the frequencies of peaks 4 and 5 increase monotonically with increasing temperature. The change in peak 4 can be attributed to the rising GeTe content in the $GeTe_{4-n}Ge_n$ ($n = 1, 2$) tetrahedra, which indicates that the tetrahedra transform into defective octahedra. The change in peak 5 is mainly due to the substitution of Sb atoms for Te atoms in $(Te_2)Sb–Sb(Te_2)$ or $(Te_2)Sb–Sb(TeSb)$ and similar structures. Due to the substitution of Te atoms by Sb atoms, the number of Te atoms increases, which leads to the formation of more $GeTe_4$ tetrahedra. Then the A_1 mode of corner-sharing $GeTe_4$ tetrahedra vibrations is enhanced. Therefore, it is observed that the intensity of peak 3 increases with increasing temperature. Meanwhile, the intensity of peak 5 prominently decreases, which can be attributed to the disappearance of the A_1 mode of $GeTe_4$ edge-sharing tetrahedra vibrations. The second variation in frequency (peak 6)

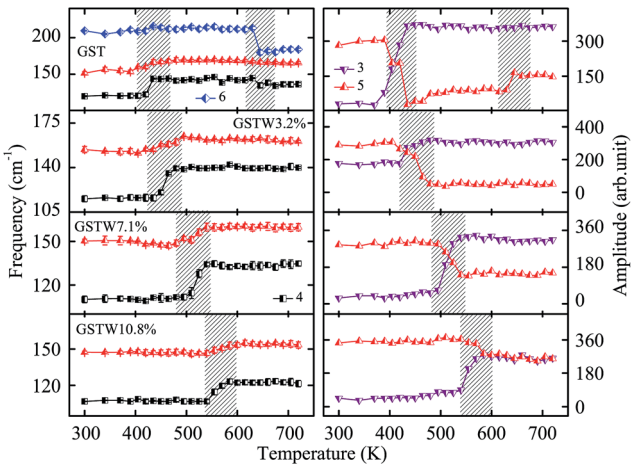

Fig. 4 Frequency variations of peak 4 and peak 5 of GSTW, and peak 4, peak 5 and peak 6 of GST as a function of temperature (left). Strength variations of peak 3 and peak 5 of GST and GSTW as a function of temperature (right). Note that the shadow patterns correspond to the phase change regions.

and intensity (peak 5) in GST can be assigned to the phase change from the FCC to HEX structure.

From the aforementioned discussion of the Raman spectra, it can be concluded that the dominant phase change mechanism of GST from amorphous to FCC structure is the change of the local banding arrangement of Ge atoms, namely from tetrahedral coordination to octahedral coordination. Although the most intense peaks are dominated by Sb_2Te_3 units, the GeTe component is mainly responsible for the phase change in the GST film. Besides this, most of the W atoms enter into the crystal lattice as substitutional impurities, while a small amount of W atoms are regarded as interstitial impurities. The impurities lead to a disorder of the crystalline structure and inhibit further crystallization. Eventually, the T_c of the GSTW films increases, which leads to an improvement in the thermal stability of the amorphous state.

4 Conclusion

In summary, temperature dependent Raman spectra were systemically studied for the analysis of the crystallization mechanism from amorphous to FCC structure of GSTW films. The average coordination of the Ge atoms increasing from fourfold to sixfold dominates the phase change from the amorphous state to FCC geometry. The W doping can lead to a higher crystallization temperature, better thermal stability of the amorphous state and higher 10 year data retention ability than pure GST film. The GSTW7.1% film possesses great potential for phase change materials.

Acknowledgements

This work was financially supported by the Major State Basic Research Development Program of China (grant nos. 2011CB922200 and 2013CB922300), Natural Science Foundation of China (grant nos. 11374097 and 61376129), Projects of Science and Technology Commission of Shanghai Municipality (grant nos. 14XD1401500, 13JC1402100 and 13JC1404200), and the Program for Professor of Special Appointment (Eastern Scholar) at Shanghai Institutions of Higher Learning.

Notes and references

1 S. R. Ovshinsky, *Phys. Rev. Lett.*, 1968, **21**, 1450.
2 N. Yamada, E. Ohno and K. Nishiuchi, *J. Appl. Phys.*, 1991, **69**, 2849.
3 A. V. Kolobov, P. Fons, A. I. Frenkel, A. L. Ankudinov, J. Tominaga and T. Uruga, *Nat. Mater.*, 2004, **3**, 703–708.
4 M. Wuttig and N. Yamada, *Nat. Mater.*, 2007, **6**, 824–832.
5 D. Lencer, M. Salinga, B. Grabowski, T. Hickel, J. Neugebauer and M. Wuttig, *Nat. Mater.*, 2008, **7**, 972–977.
6 X. L. Zhou, L. C. Wu, Z. T. Song, F. Rao, B. Liu, D. N. Yao, W. J. Yin, J. T. Li, S. L. Feng and B. Chen, *Appl. Phys. Express*, 2009, **2**, 091401.
7 D. J. Milliron, S. Raoux, R. M. Shelby and J. Jordan-Sweet, *Nat. Mater.*, 2007, **6**, 352–356.
8 F. Rao, K. Ren, Y. F. Gu, Z. T. Song, L. C. Wu, X. L. Zhou, B. Liu, S. L. Feng and B. Chen, *Thin Solid Films*, 2011, **519**, 5684–5688.
9 H.-Y. Cheng, S. Raoux and J. L. Jordan-Sweet, *Appl. Phys. Lett.*, 2011, **98**, 121911.
10 K. S. Andrikopoulo, S. N. Yannopoulos, G. A. Voyiatzis, A. V. Kolobov, M. Ribes and J. Tominaga, *J. Phys.: Condens. Matter*, 2006, **18**, 965–979.
11 S. Caravati, M. Bernasconi and M. Parrinello, *Phys. Rev. B: Condens. Matter Mater. Phys.*, 2010, **81**, 014201.
12 Y. K. Kim, K. Jeong, M. H. Cho, U. Hwang and H. S. Jeong, *Appl. Phys. Lett.*, 2007, **90**, 171920.
13 S. Privitera, E. Rimini and R. Zonca, *Appl. Phys. Lett.*, 2004, **85**, 3044.
14 W. D. Song, L. P. Shi, X. S. Miao and T. C. Chong, *Appl. Phys. Lett.*, 2007, **90**, 091904.
15 B. Prasai, G. Chen and D. A. Drabold, *Appl. Phys. Lett.*, 2013, **102**, 041907.
16 X. N. Cheng, F. X. Mao, Z. T. Song, C. Peng and Y. F. Gong, *Jpn. J. Appl. Phys.*, 2014, **53**, 050304.
17 C. Peng, L. C. Wu, F. Rao, Z. T. Song, P. X. Yang, H. J. Song, K. Ren, X. L. Zhou, M. Zhu, B. Liu and J. H. Chu, *Appl. Phys. Lett.*, 2012, **101**, 122108.
18 W. A. Johnson, *Membrane Structure and Mechanisms of Biological Energy Transduction*, Springer US, 1973, pp. 559–583.
19 K. F. Kao, C. M. Lee, M. J. Chen, M. J. Tsai and T. S. Chin, *Adv. Mater.*, 2009, **21**, 1695.
20 J. Hegedüs and S. R. Elliott, *Nat. Mater.*, 2008, **7**, 399–405.
21 A. V. Kolobov, P. Fons and J. Tominaga, *Appl. Phys. Lett.*, 2003, **82**, 382.
22 S. Caravati and M. Bernasconi, *Appl. Phys. Lett.*, 2007, **91**, 171906.
23 T. Matsunaga, N. Yamada and Y. Kubota, *Acta Crystallogr., Sect. B: Struct. Sci.*, 2004, **60**, 685–691.
24 P. Nemec, V. Nazabal, A. Moreac, J. Gutwirth, L. Benes and M. Frumar, *Mater. Chem. Phys.*, 2012, **136**, 935–941.
25 G. C. Sosso, S. Caravati and M. Bernasconi, *J. Phys.: Condens. Matter*, 2009, **21**, 095410.
26 R. Mazzarello, S. Caravati, S. Angioletti-Uberti, M. Bernasconi and M. Parrinello, *Phys. Rev. Lett.*, 2010, **104**, 085503.

